GSA Data Repository 2018047
Rahl et al., 2018, Rhomb-dominated crystallographic preferred orientations in incipiently deformed quartz sandstones: A potential paleostress indicator for quartz-rich rocks: Geology, https://doi.org/10.1130/G39599.1.

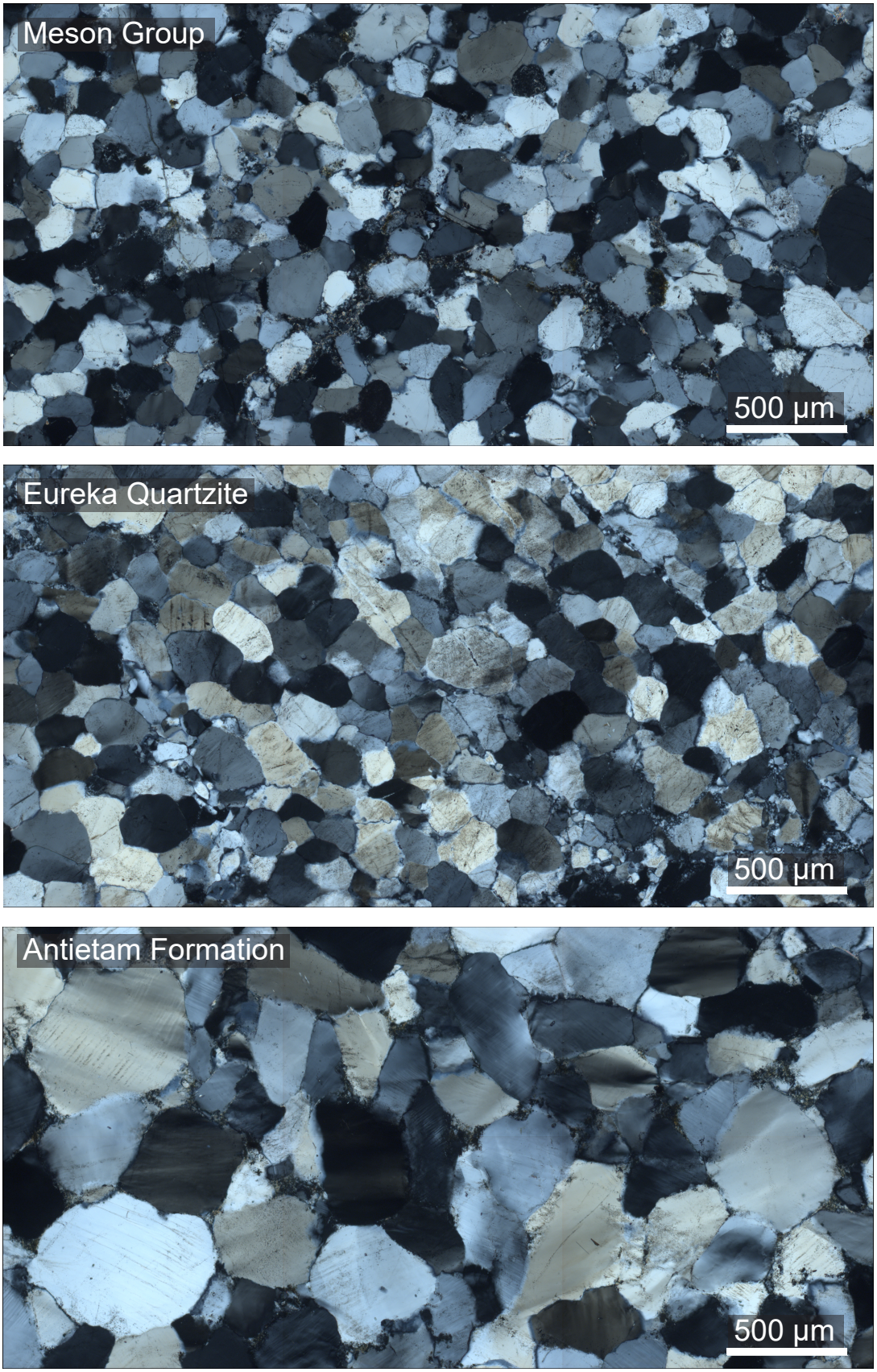

Figure DR1. Representative photomicrographs of the sample materials, quartzites from the Meson Group, Eureka Quartzite, and Antietam Formation (top to botom).

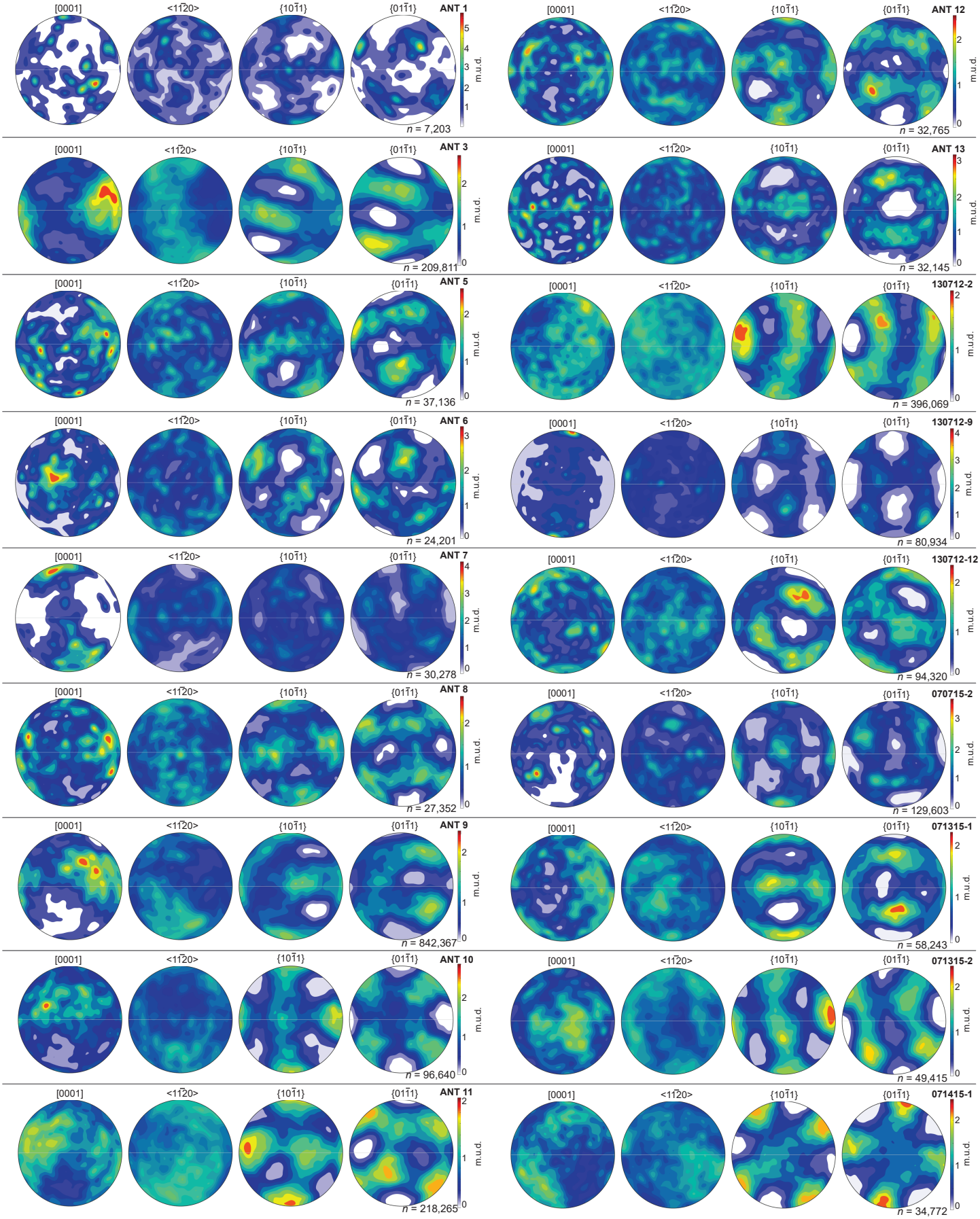

Figure DR2. Pole figures of contoured bulk quartz crystallographic data (n = total number of observations). Step size for analytical runs shown in Table DR1. The pole to the bedding plane (P2B) is oriented along the N-S axis and an arbitrary direction aligned E-W. Orientations shown are for [0001] (c-axis), <11-20> (a-axis), <10-11> (positive rhomb, r), and <01-11> (negative rhomb, z) directions. m.u.d. = multiples of uniform density. These data show discernable maxima in the rhombs are observable even when c-axis distributions are uniform or show only very weak maxima.

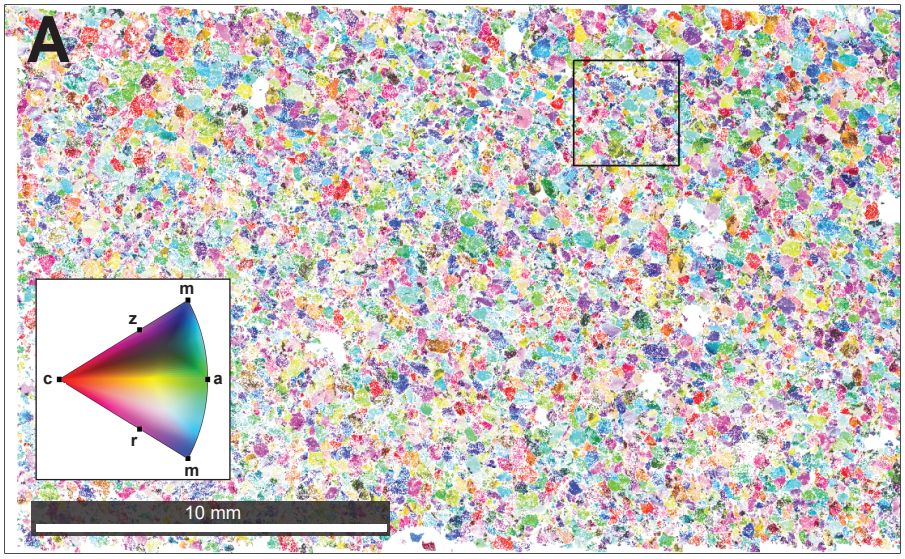

ANT 9, Antietam Formation

n = 842,367

130712-2, Meson Group

n = 396,069

071315-2, Pequop Mountains

n = 49,415

Figure DR3. Representative large area quartz crystallographic maps, collected using a rectangular grid with a 30 µm step size. Data are colored according to the inverse pole figure (IPF) for quartz for the direction oriented perpendicular to the long axis of the thin section (i.e., for the N-S direction in the map). The bedding plane is oriented E-W, with the pole to bedding on the N-S axis. The IPF key is inset in A. Maps on the left (A, C, E) show the large datasets from which the pole figures like those in Figure 1 or DR2 were constructed. Maps on the right (B, D, F) show zoomed views of the outlined areas in the larger maps, showing that the large datasets have sufficient resolution to identify both grains and twins.

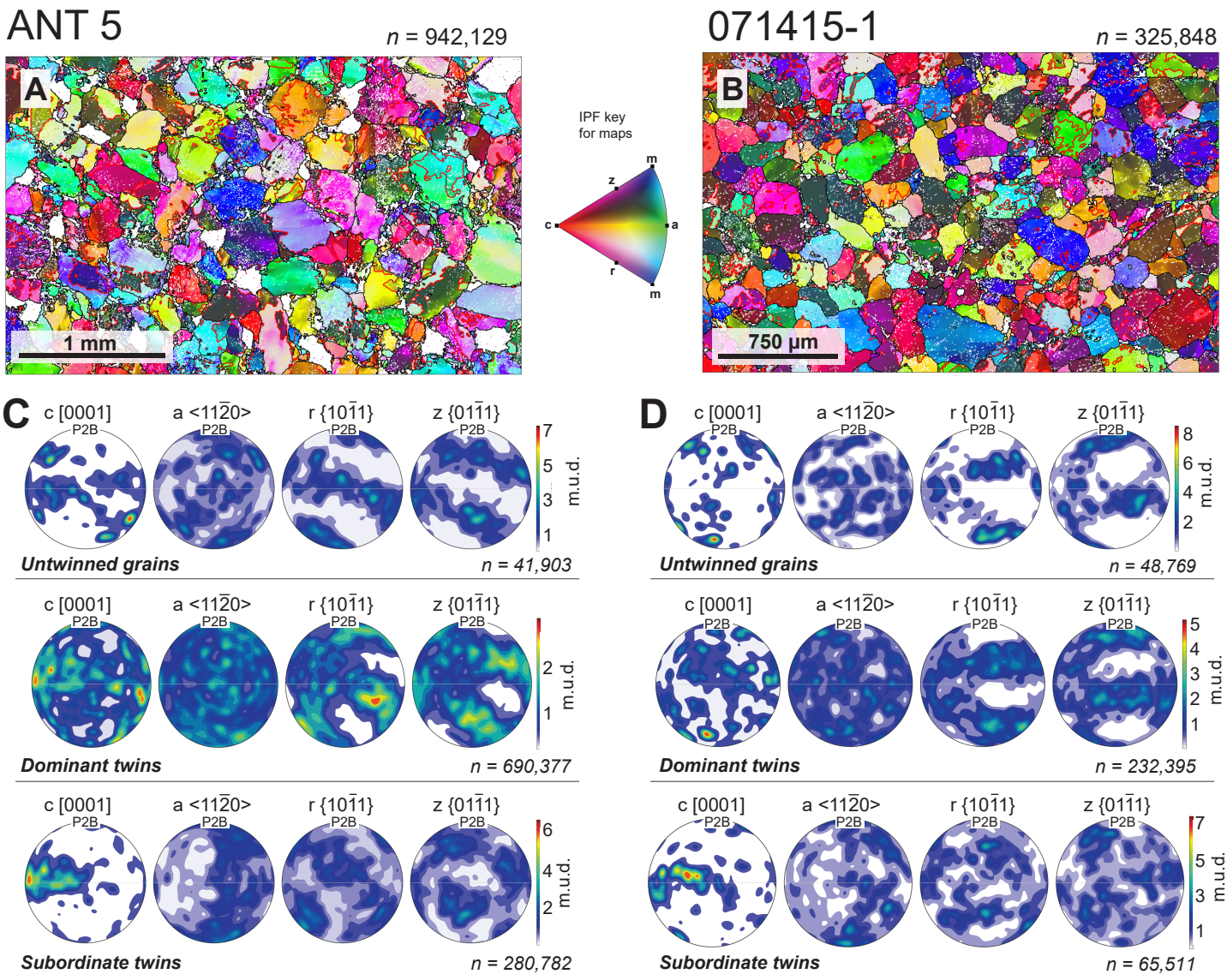

Figure DR4. Quartz crystallographic data from samples ANT 5 of the Antietam Formation (left) and 071415-1 of the Eureka Quartzite, collected on a rectangular grid with a 5 µm step size. The data was collected on thin sections cut perpendicular to bedding. Data in maps (A and B) are colored according to the inverse pole figure (IPF) for quartz (center) for the y-direction in the maps. Grain boundaries shown in black; red lines indicate Dauphiné twin boundaries, identified by a 60 ± 2.5° rotation misorientation around [c]. C,D: Pole figures of contoured quartz crystallographic data, for data from untwinned grains (upper), the volumetrically dominant twins (middle), and the subordinate twins (lower). Contoured data include all collected data (*n* = number of observations). The pole figures are oriented with the pole to bedding (P2B) on the N-S axis (the y-direction on the map) and an arbitrary direction on the E-W axis (the x-direction on the map). Orientations shown are for [0001] (c-axis), <11-20> (a-axis), {10-11} (positive rhomb, r), and {01-11} (negative rhomb, z) directions. m.u.d. = multiples of uniform density.

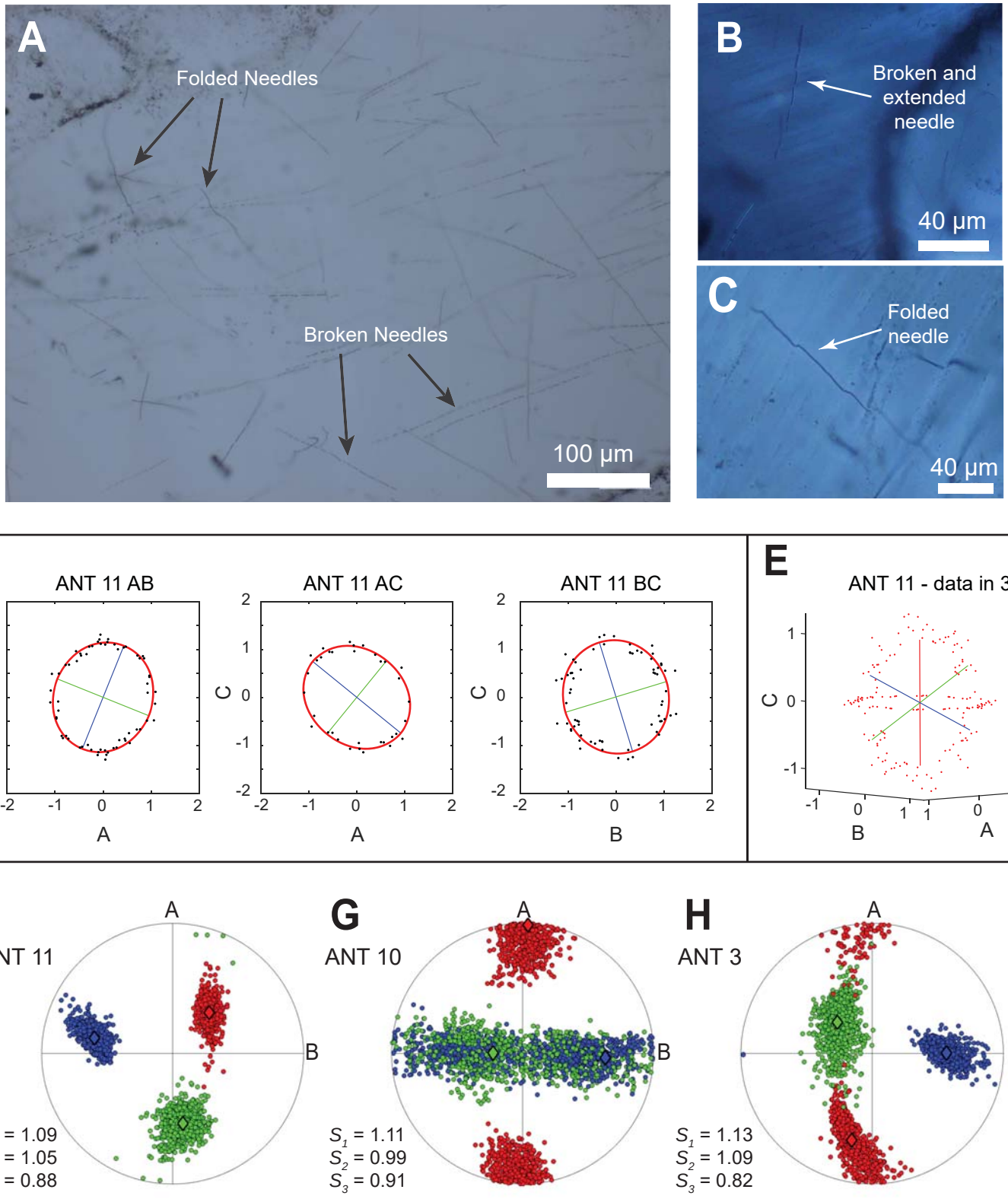

Figure DR5. A) Plane-polarized light image showing quartz crystal with numerous deformed needle-like inclusions of rutil, Antietam Formation. B,C) Cross-polarized image of deformed rutile needles from the Antietam Formation. D) Strain data from rutile inclusions for sample ANT 11, showing the stretch value and orientation of each observation (points) as well as best-fit 2D ellipse. The reference axes A, B, and C correspond to the bedding dip direction, the pole to the bedding plane, and the bedding strike direction, respectively. E) 3d plot showing the stretch and orientation values for the strain data. F-H) Solutions for the finite strain ellipsoid from the 3D strain analysis for three samples from the Antietam Formation, plotted in pole figures in A,B,C reference frame. The diamonds represent the positions of the finite strain axes (blue = S_3, green = S_2, red = S_1); the circles show the calculated solutions for 1000 bootstrap replicate datasets.

Table A1 – sample location and electron backscatter diffraction scan data

Sample	Area	UTM Zone	Easting	Northing	Unit	Step size (microns)	Scanned area (sq mm)
ANT 1	Blue Ridge, VA	17S	648147	4181048	Antietam Formation	30	79.8
ANT 3	Blue Ridge, VA	17S	650192	4185559	Antietam Formation	25	86.3
ANT 5	Blue Ridge, VA	17S	645728	4175740	Antietam Formation	30	82.9
ANT 6	Blue Ridge, VA	17S	634664	4158934	Antietam Formation	30	60.2
ANT 7	Blue Ridge, VA	17S	692423	4225890	Antietam Formation	25	54.6
ANT 8	Blue Ridge, VA	17S	694920	4236680	Antietam Formation	30	60.2
ANT 9	Blue Ridge, VA	17S	703217	4245533	Antietam Formation	30	58.2
ANT 10	Blue Ridge, VA	17S	634941	4160495	Antietam Formation	30	58.2
ANT 11	Blue Ridge, VA	17S	659440	4196271	Antietam Formation	30	58.2
ANT 12	Blue Ridge, VA	17S	639067	4168687	Antietam Formation	30	58.2
ANT 13	Blue Ridge, VA	17S	634698	4163025	Antietam Formation	30	58.2
130712-9	NW Argentina	20K	283298	-7511814	Meson Group	40	330.7
130712-2	NW Argentina	20K	277934.6	-7516555	Meson Group	25	382.7
130712-12	NW Argentina	20K	283455.9	-7511058	Meson Group	40	451.0
070715-2	Pequop Mtns	11N	698603	4534046	Prospect Mountain Quartzite	25	230.6
071315-1	Pequop Mtns	11N	699657	4530124	Kanosh Sandstone	20	85.2
071315-2	Pequop Mtns	11N	700637	4530453	Eureka Quartzite	50	328.0
071415-1	Pequop Mtns	11N	707836	4543924	Eureka Quartzite	50	366.9